



HAL
open science

3D-printed lab-on-valve for fluorescent determination of cadmium and lead in water

Elodie Mattio, Fabien Robert-Peillard, Laurent Vassalo, Catherine Branger, André Margaillan, Christophe Brach-Papa, Joel Knoery, Jean-Luc Boudenne, Bruno Coulomb

► To cite this version:

Elodie Mattio, Fabien Robert-Peillard, Laurent Vassalo, Catherine Branger, André Margaillan, et al.. 3D-printed lab-on-valve for fluorescent determination of cadmium and lead in water. *Talanta*, 2018, 183, pp.201-208. 10.1016/j.talanta.2018.02.051 . hal-01737459

HAL Id: hal-01737459

<https://amu.hal.science/hal-01737459v1>

Submitted on 18 Apr 2018

HAL is a multi-disciplinary open access archive for the deposit and dissemination of scientific research documents, whether they are published or not. The documents may come from teaching and research institutions in France or abroad, or from public or private research centers.

L'archive ouverte pluridisciplinaire **HAL**, est destinée au dépôt et à la diffusion de documents scientifiques de niveau recherche, publiés ou non, émanant des établissements d'enseignement et de recherche français ou étrangers, des laboratoires publics ou privés.

1 **3D-printed lab-on-valve for fluorescent determination of cadmium and lead in water**

2

3 Elodie Mattio¹, Fabien Robert-Peillard¹, Laurent Vassalo¹, Catherine Branger², André

4 Margaillan², Christophe Brach-Papa³, Joël Knoery³, Jean-Luc Boudenne¹, Bruno Coulomb^{1*}

5 ¹ Aix Marseille Univ, CNRS, LCE, Marseille, France.

6 ² University of Toulon, MAPIEM, La Garde, France.

7 ³ IFREMER, LBCM, Nantes, France.

8

9 *Corresponding author: bruno.coulomb@univ-amu.fr

10 Full postal address: LCE, Case 29, 3 place Victor Hugo, 13331 Marseille cedex 3, France.

11

12 **Abstract**

13 In recent years, the development of 3D printing in flow analysis has allowed the creation of
14 new systems with various applications. Up to now, 3D printing was mainly used for the
15 manufacture of small units such as flow detection cells, preconcentration units or mixing
16 systems. In the present study, a new 3D printed lab-on-valve system was developed to
17 selectively quantify lead and cadmium in water. Different technologies were compared for lab-
18 on-valve 3D printing. Printed test units have shown that stereolithography or digital light
19 processing are satisfactory techniques for creating complex lab-on-valve units. The lab-on-
20 valve system was composed of two columns, eight peripheral ports and a central port, and a
21 coil integrating baffles to increase mixing possibilities. A selective extraction of lead was first
22 carried out by TrisKem PbTM Resin column. Then, cadmium not retained on the first column
23 was extracted on a second column of Amberlite® IR 120 resin. In a following step, lead and
24 cadmium were eluted with ammonium oxalate and potassium iodide, respectively. Finally, the
25 two metals were sequentially detected by the same Rhod-5NTM fluorescent reagent. This 3D

1 printed lab-on-valve flow system allowed us to quantify lead and cadmium with a linear
2 response from 0.2 to 15 $\mu\text{g.L}^{-1}$ and detection limits of 0.17 and 0.20 $\mu\text{g.L}^{-1}$ for lead and
3 cadmium, respectively, which seems adapted for natural water analysis.

4

5 Keywords: stereolithography; digital light processing; LOV-MSFIA; natural waters

6

7 **Introduction**

8 Cadmium and lead are two of the most concerning metals in water in the light of their toxicities
9 and their levels in the environment. Many pollution sources can cause increased levels of Cd
10 and Pb: natural sources like volcanic activity [1] and anthropogenic sources which represent
11 the most important impact, such as metallurgy [2], mining operation [3], electronic industry [4],
12 pesticides [5], or even paints [6].

13 These metals have several impacts on health: cadmium has a half-life in humans of 10 to 35
14 years [7] and is mainly accumulated in kidney and liver which might lead to deficiencies [8]
15 like the Itai-itai disease, but it can also be found in spleen, brain and blood, resulting in
16 increasing cancers risks. Lead intoxication can lead to many dysfunctions like cardiovascular
17 diseases [9], neurodevelopmental effects or impaired fertility [10]. In the light of these effects,
18 the World Health Organization has recommended a guideline value of 3 $\mu\text{g.L}^{-1}$ and 10 $\mu\text{g.L}^{-1}$
19 for cadmium and lead respectively in drinking water.

20 Accordingly, the development of simple, rapid and sensitive methods for on-line and on-site
21 Cd and Pb determination in natural waters has attracted widespread attention in modern
22 analytical chemistry.

23 Flow analysis seems to be appropriate for the development of these type of portable analytic
24 systems: this technology allows decreasing instrumentation size, and reagents and energy

1 consumption, which are significant advantages for an on-site system while simplifying the
2 manipulations required for the assays.

3 Many flow systems with minimal interferences and low detection limits have been developed
4 for the quantification of cadmium and lead in natural waters but most of these systems are
5 coupled with inductively coupled plasma spectroscopy [11] or atomic absorption spectrometry
6 [12,13], detection techniques that are not compatible with portable systems.

7 Sequential Injection-Lab-on-valve (SI-LOV) flow systems, developed by Ruzicka [14], allow
8 one to integrate the various steps of an analytical method in a miniaturized part placed on the
9 head of a selection valve. The lab-on-valve improves repeatability, reliability and robustness of
10 flow systems while being more compact thus facilitating on-site measurements. Some SI-LOV
11 systems have been developed for solid phase extraction and solid phase detection of metals [15-
12 17]. For lead and cadmium determination, a SI-LOV system has recently been described [18]
13 but the limits of detection ($34 \mu\text{g.L}^{-1}$ and $56 \mu\text{g.L}^{-1}$ for cadmium and lead respectively) limit the
14 use of the system to a rapid screening of the two metals in contaminated waters.

15 Until now, the possibilities of LOV creation have been limited by the machining of parts by
16 drilling, embossing or molding, which does not make it possible to integrate all the analysis
17 steps in the LOV. This problem henceforth can be solved by using 3D printing.

18 3D printing enables one to create three-dimensional object from computer-aided design model
19 by using different printing technologies, and is increasingly used in flow analysis to create
20 tailor-made units: an experimental comparison of three 3D printing technologies used in flow
21 analysis has been carried out to evaluate best performances [19], and many reviews resume
22 emerging applications of 3D printing in microfluidic systems [20-22]. A MSFIA system has
23 recently been developed for the iron speciation with a 3D printed device integrating analyte
24 oxidation, disk-based SPE and analyte complexation [23].

1 Fused Deposition Modeling (FDM) and photo-polymerization processes such as
2 Stereolithography (SLA), Digital Light Processing (DLP) and Polyjet® are the main 3D
3 printing technologies used in flow systems. In SLA and DLP technologies, a unit is created
4 layer by layer from a photopolymer resin, cured by a UV-laser (SLA) or a conventional light
5 source (DLP). SLA and DLP enable formation of units directly in the liquid photopolymer resin
6 tank on a platform that goes up as the layers are printed. In Polyjet® technology, the liquid
7 material is deposited on a build platform and is cured, by the passage of an UV lamp layer after
8 layer. This technology requires the use of a water-soluble support material to fill the voids
9 (tubing, cells, and columns) of the part during printing. This water-soluble support material is
10 then cleaned during post-processing of the printed part.

11 In this paper, a new 3D printed lab-on-valve is presented and integrated in a MSFIA system for
12 the determination of low levels of Cd and Pb in natural waters. The 3D-printed LOV is
13 constituted of 8 peripheral ports and a central port connected to the 3-way valve of a syringe
14 and contains two columns used for solid phase extraction and preconcentration of lead and
15 cadmium, a mixing coil with baffles to break flow and increase turbulences in order to increase
16 mixing capabilities, and a fluorescence detection cell. The analytical procedure developed is
17 first based on the selective extraction of lead by the TrisKem Pb resin® (this resin has been
18 already studied and included in a 3D-printed flow system for determination of lead in natural
19 waters in a previous study [24]). In a second step, cadmium is extracted on Amberlite® IR 120
20 exchange resin and selectively eluted with potassium iodide. The quantification of the two
21 metals is based on the use of the Rhod-5N™ fluorescent reagent. The MSFIA-LOV developed
22 system has been validated on real river water samples.

23

24 **2. Materials and methods**

25 2.1. Reagents

1 All chemicals used were of analytical grade and used without further purification. Solutions
2 were prepared with ultra-pure water (Millipore, resistivity > 18 MΩ cm) and stocked in high
3 density polyethylene or Teflon flasks. Cadmium and lead standard solutions were prepared by
4 dilution of commercial 1 g.L⁻¹ AAS stock solutions (Fisher Chemical, USA) and stabilized with
5 1% v/v nitric acid trace metal grade (Fisher Chemical, USA). Calcium solution was prepared
6 by dissolving anhydrous calcium chloride (Alfa Aesar, Germany) in ultra-pure water. A multi-
7 metal solution (10 μmol.L⁻¹ for each metal) was prepared by diluting and mixing eleven
8 commercial AAS stock solutions of aluminium, cadmium, calcium, cobalt, chromium, copper,
9 iron, lead, magnesium, nickel and zinc, at 1 g.L⁻¹ (Fisher Chemical, USA) in ultra-pure water.
10 Cadmium and lead extraction were respectively carried out with the Amberlite® IR 120
11 Hydrogen Form resin (Prolabo, France) and the TrisKem Pb Resin (PB-B25-S, 50-100μm,
12 TrisKem, France). Eluents were prepared from potassium iodide (Sigma-Aldrich, USA) for
13 cadmium and from ammonium oxalate (Prolabo, France) for lead. Other eluents tested were
14 prepared from trace metal grade nitric acid (Fisher Chemical, USA) and ammonium nitrate
15 (Prolabo, France).
16 For detection, a 0.2 μmol.L⁻¹ solution of Rhod-5N tripotassium salt (Fisher Chemical, USA)
17 was prepared in a 10 mmol.L⁻¹ 3-(N-morpholino)propanesulfonic acid (MOPS) buffer solution
18 at pH = 7 (Sigma-Aldrich, USA). To take into account the interferences related to the presence
19 of calcium in the samples, a two-step analytical procedure was developed and required the
20 addition of a 3 μmol.L⁻¹ masking agent solution of N,N,N',N'-tetrakis-(2-
21 pyridylmethyl)ethylenediamine (TPEN) (Sigma-Aldrich, USA) to the Rhod-5N reagent.

22

23 2.2. Apparatus

24 2.2.1. Metal analysis

1 The extraction and elution steps of cadmium, lead and interfering metals on TrisKem Pb resin
2 and Amberlite® IR 120 resin were studied by inductively coupled plasma–atomic emission
3 spectrometry (ICP–AES) with a Jobin YVON JY2000 Ultratrace spectrometer, equipped with
4 a CMA spray chamber and a Meinhard R50-C1 glass nebuliser. Determinations were performed
5 with the following settings: power 1000W, pump speed 20 mL.min⁻¹, plasma flow rate 12
6 L.min⁻¹, coating gas flow rate 0.15 L.min⁻¹, nebuliser flow rate 1.08 L.min⁻¹ and nebuliser
7 pressure 2.6 bar.

8 Graphite furnace atomic absorption spectrometry (GF-AAS) was used to quantify lead in real
9 samples. The measurements were carried out on a Thermo Scientific ICE3500 (USA) atomic
10 absorption spectrometer equipped with a lead hollow-cathode lamp operated at 10 mA
11 (wavelength of 217 nm). Argon flow was 0.2 L.min⁻¹ except during atomisation step (no flow).
12 The furnace settings were as follow: drying at 110 °C, ramp for 9 s, hold for 35 s; cracking at
13 800 °C, ramp for 5 s, hold for 20 s; atomising at 1200 °C, ramp for 1 s and 3 s hold; cleaning at
14 2500 °C, no ramp and 3 s hold.

15

16 2.2.2. *Flow system*

17 The MSFIA-LOV system used in this study is shown in Fig. 1. Different LOV units were
18 designed with Rhinoceros® 5.0 3D software (Robert McNeel & Associates Europe, Spain).
19 Various 3D printers were tested to fabricate units: the Form1+ printer (Formlabs, USA), the
20 Object500 Connex 3 printer (Stratasys, USA) and the Miicraft 100 printer (Miicraft, Rays
21 Optics Inc., Taiwan). The three printers were used with acrylic transparent resins that had
22 chemical resistance properties closed to those of poly(methyl methacrylate) (PMMA) with good
23 resistance to common diluted acids. The 3D printed LOV part was fixed on an 8-ports
24 multiposition selection valve module (Sciware Systems SL, Spain) and coupled with a
25 multisyringe burette module with programmable speed (Multiburette 4S, Crison Instruments,

1 Spain) equipped with three 5 mL glass syringes (Hamilton, Switzerland). Each syringe was
2 connected to a 3-way solenoid valve (S1, S2, S3) for multicommutation steps. A continuous
3 renewal of sample was done by a solenoid micro-pump (Bio-ChemValve Inc., USA) that had a
4 stroke volume of 20 μL and a high frequency of 250 $\text{cycles}\cdot\text{min}^{-1}$.

5 For the detection, a Kontron Instruments SFM25 fluorometer (Kontron, Germany) was used
6 with a HellmaTM quartz UV flow cell. It should be noted that the spectrofluorimeter used in this
7 study can be easily replaced by a more compact detection system based on the use of a laser
8 diode for excitation and a photodiode for detection.

9 The whole system, except the fluorometer, was controlled by AutoAnalysis 5.0 software
10 (Sciware Systems SL, Spain).

11

12 2.3. Lab-on-valve unit

13 The LOV had the following dimensions: height 66 x width 100 x depth 17 mm. It was composed
14 by eight peripheral ports and a central port connected to S1 via a holding coil (Figure 1).
15 Channel inner diameters were 1.2 mm, except for mixing coil which was 0.8 mm i.d. at the
16 narrowest point. Two ports (1 and 2) were externally linked on the top of columns (C1 and C2)
17 by a 0.8 mm i.d. PTFE tubing to introduce sample and reagents. Both columns were 3D printed
18 and were independent of the LOV system so that they could be easily changed (the two columns
19 were simply screwed to two LOV inputs). C1 and C2 were respectively filled with 50 mg of
20 TrisKem Pb resin for lead extraction and 50 mg of Amberlite[®] IR 120 for cadmium
21 preconcentration. These columns were linked to a 184 mm long mixing coil (connected to the
22 detector via port 8). This mixing coil was designed with 2 mm wide baffles in order to break
23 flow and increase turbulences, therefore increasing mixing capabilities of the coil. A two-way
24 microconduit allowed the introduction of detection reagents.

1 Ports 3 and 7 were employed for sample introduction and waste, respectively. The remaining
2 peripheral ports (port 4, 5 and 6) were used for the introduction of the eluents: nitric acid (4),
3 ammonium oxalate (5) and potassium iodide (6).

4

5 2.4. Analytical procedure

6 The complete analytical sequence for cadmium and lead preconcentration and detection is listed
7 in Table 1 and can be summarized as follows:

- 8 1. Conditioning of TrisKem Pb resin with HNO_3 0.05 mol.L^{-1} : the central port (CC) of the
9 LOV is connected to the peripheral port 4 to aspirate 4 mL of nitric acid in holding coil
10 (HC) which are propelled towards C1 via port 1.
- 11 2. Sample introduction: the sample is loaded in HC (port 3) and then dispensed towards
12 C1 (port 1) at a flow rate of 4 mL.min^{-1} . Once the lead retained onto TrisKem Pb resin
13 (C1), this lead-extracted sample is reaspirated via port 8 in the HC and dispensed
14 through C2 (port 2) for cadmium extraction on the Amberlite® IR 120.
- 15 3. Elution and detection of cadmium: potassium iodide (0.15 mol.L^{-1}) and Rhod-5N (0.2
16 $\mu\text{mol.L}^{-1}$) are simultaneously dispensed respectively through C2 (port 2) to eluate
17 extracted cadmium and at the inlet of the mixing coil (S2). Measurement is based on the
18 peak height with $\lambda_{\text{ex}} = 550 \text{ nm}$ and $\lambda_{\text{em}} = 575 \text{ nm}$.
- 19 4. Second introduction of sample: steps 3 to 6 are repeated. A total volume of 10 mL is
20 thus dispensed through the TrisKem Pb resin (C1). The aim of this second sample
21 introduction is to quantify interference of calcium for cadmium determination. During
22 the detection step, potassium iodide (port 6) solution and Rhod-5N+TPEN reagent (S3)
23 are simultaneous dispensed. TPEN is added to Rhod-5N reagent to complex cadmium
24 and detect calcium specifically. The interference generated by calcium can thus be
25 determined.

1 5. Elution and detection of lead: the TrisKem Pb resin (C1) is washed with nitric acid
2 solution (0.05 mol.L⁻¹) to eliminate potential interfering species extracted by the resin.
3 Ammonium oxalate solution (0.025 mol.L⁻¹) and Rhod-5N are simultaneously
4 dispensed to eluate and detect lead.

6 **3. Results and discussion**

7 3.1. 3D printing of the LOV unit

8 The first step to print a lab-on-valve, after its conception on a 3D software, was to select a
9 suitable technology. The printing of LOV units requires a good resolution on the 3 axes XYZ
10 and a high precision. Several printers have thus been tested to find the most suitable for the
11 manufacture of LOV units.

12 Fused Deposition Modeling (FDM), the most used technology in 3D printing, is not suitable
13 for creating fluidic systems, in the light of difficulties to form small tubings and smooth surface
14 without post-treatment. The same statement could be done with Selective Laser Sintering
15 (SLS), in which the grain size of powdered materials limits the resolution and gives a porous
16 unit.

17 Photopolymerisation technologies are therefore recommended for LOV printing:
18 stereolithography (SLA), digital light processing (DLP) and Polyjet® technology provide
19 sufficient performance to print complex flow units. These three technologies were therefore
20 studied to print the LOV unit used in this study. Figure 2 shows photos of the printed LOV
21 units.

23 *3.1.1. Polyjet® technology*

24 Several LOV units have been printed with Polyjet® technology using an Object500 Connex 3
25 printer, a Veroclear® transparent acrylic/epoxy resin and a SUP706 soluble support material

1 (Stratasys, USA). Considering the high cost of the printer (more than 200 k€), the fabrication
2 of the piece was subcontracted to a specialized company (Maquette74, France). In this
3 technique, photopolymer drops are deposited and cured by an UV lamp and the printing of
4 micro conduits of LOV unit requires a water-soluble support material. Three 3D-printed LOV
5 units have been compared: one without mixing coil, one with classical coil, and another with a
6 mixing coil containing baffles, to increase turbulences and mixing capacities.

7 The two LOV units with mixing coils had clogging problems (Figures 2.1 and 2.3). Note that
8 in figures 2.1 and 2.3 the photos have been retouched and the clogged parts have been contrasted
9 in red for a better understanding. In the black and white version of the photos, the clogged
10 tubing sections appear lighter than the properly formed tubings. Original unretouched photos
11 are presented in supplementary materials (Fig. S1). In these printed LOV units, water-soluble
12 support could not be completely removed at the end of printing processing, even with
13 mechanical (brushing) or chemical treatment (solubilisation by NaOH solution). The cleaning
14 of coil tubing (with or without baffles) was very difficult and tubings remained clogged after
15 printing and cleaning.

16 However, the LOV unit without mixing coil did not have clogging problems: channels were
17 clean and the surface unit was smooth, which was an advantage for the area in contact with the
18 Teflon disk in order to limit leaks. Therefore, Polyjet® technology could be recommended to
19 print simple LOV units, without mixing coil or complex tubings, because of its high precision,
20 the robustness of printed pieces and its high quality finish.

21

22 *3.1.2 Stereolithography*

23 The Form1+ printer has been used in lab to evaluate performances of stereolithography to print
24 a LOV unit. This printer costs about 3.5 k€ and the units were printed with clear acrylic resin

1 FLGPCL02. In this technology, the unit is formed directly in the tank of the liquid
2 photopolymer and water-soluble support is thus not required to form tubing.
3 The same three LOV units were 3D printed by stereolithography (resolution of 100 μm , printing
4 time 6 hours) using the same .stl files previously used with Polyjet® technology printing. The
5 results did not show any clogging problem (Figure 2.2). The eight positions of the LOV were
6 correctly formed, however the surface was uneven and many defects were observed at several
7 layers of the units resulting in microcracks in the printed part.
8 Furthermore, deformations of printed units were observed: this problem is frequently
9 encountered in SLA due to resin shrinkage, which causes leaks between the positions of the
10 LOV, and furthermore, optical pathlengths may exhibit significant deformation preventing
11 optimal detection. Some printer software can take this issue into account by proposing X and
12 Y axis compensation, but this parameter was not found in the Preform software used to control
13 the Form1+. A smaller resolution was able to improve the precision of LOV positions (25 or
14 50 μm), but the printing time was longer (20 and 10 hours respectively) which could increase
15 the risk of printing problems like unit's fall in resin tank or incomplete formation. Unsuccessful
16 printing tests with 25 and 50 μm resolution led us to limit the resolution to 100 μm for lab-on-
17 valve fabrication. Besides, a post-treatment was necessary to obtain a real smooth area in
18 contact with the Teflon disk of the selection valve.

19

20 *3.1.3. Digital light processing (DLP)*

21 The disadvantages of previous technologies to print the designed LOV unit led us to study
22 digital light processing. For this technology, the unit formation is the same as in
23 stereolithography, however the resin is not progressively photo-polymerized by a laser like in
24 stereolithography but a projector displays directly an UV image of each layer to photo-
25 polymerize resin on the platform.

1 Different units were printed in lab with the Miicraft 100 printer (printer price is about 10k euros)
2 and the BV-007 transparent acrylic resin: the printed parts showed a smoother surface with
3 faster printing (with a resolution of 20 μm , printing time 5 hours) than in stereolithography
4 (Figure 2.4). Moreover, tubings formation were more accurate and it has been possible to
5 decrease the inner diameter to 0.8 mm vs 1.2 mm in stereolithography. The area in contact with
6 the Teflon disk of the selection valve was perfectly formed and no leak has been observed.
7 In conclusion of this part, Figure 2 summarized the observations made for each technology: the
8 Polyjet technology® did not allow the printing of a mixing coil without clogging problem
9 (picture 1 and 3). At the opposite, the stereolithography could print an unclogged LOV unit but
10 with an uneven and harsh surface (picture 2), resulting in a bad positioning of the LOV part on
11 the valve rotor and causing leakage of the reagents used and deterioration of the Teflon disk of
12 the valve. The digital light processing gathered the advantages of the two previous technologies:
13 the printed surface was smooth and tubing were well-formed (picture 4). In these conditions,
14 DLP appeared to be the more adapted technology to print a LOV unit with mixing coil.
15 However, to work without mixing coil, the Polyjet technology® showed better performances
16 than DLP.

17

18 3.2. Lead determination

19 The procedure for lead determination in natural waters has already been described in a previous
20 study [24]. The determination was based on selective solid phase extraction of lead on a
21 commercial resin (TrisKem Pb resin) in HNO_3 0.05 mol.L⁻¹. For this study, the extraction of
22 lead has been studied at pH 7 in order to reuse the sample for cadmium determination.

23 The results showed that TrisKem Pb resin extracted lead more than 90% at pH 7, a result very
24 close to that obtained in the presence of nitric acid (Fig S2). Most of cations, including calcium
25 and magnesium, were not retained by the resin, except for iron that was partially extracted

1 (<20%). The washing step with HNO_3 0.05 mol.L^{-1} has been previously studied [24] and
2 allowed elimination of 75% of iron extracted. Lead elution was carried out by ammonium
3 oxalate 0.025 mol.L^{-1} to extract more than 90% of lead. Lead was then detected by the Rhod-
4 5N reagent and the remaining iron did not interfere in the measurement.

6 3.3. Cadmium determination

7 To measure low levels of cadmium in natural waters, a sensitive and selective reagent for
8 detection has to be used. In addition, the use of the same reagent for the detection of lead and
9 cadmium makes it possible to simplify the flow system. Several chromogenic reagents for a
10 spectrophotometric detection have been considered, like 4-(2-pyridylazo)resorcinol (PAR) or
11 dithizone, however, none of them allowed a selective detection at very low concentrations.
12 Fluorescent reagents have also been examined: 8-hydroxyquinoline-5-sulfonic acid [25] shows
13 major interferences that could disturb cadmium measurement. Rhod-5N [26] appears to meet
14 the requirements of selectivity and sensitivity and has been used in this study. Although Rhod-
15 5N has some selectivity for cadmium, some other cations can be detected with this reagent.
16 Calcium, lead, copper, iron and zinc are the main interfering cations in natural waters. In this
17 study lead is extracted beforehand by TrisKem Pb resin and copper and iron do not react with
18 Rhod-5N. These cations will not interfere in the measurement of cadmium. However, it was
19 necessary to find a resin allowing the selective extraction of cadmium to avoid calcium and zinc
20 interferences.

21 22 3.3.1. Cadmium selective preconcentration

23 Several commercial cation exchange resins have been studied. Two resins have been
24 particularly tested: an iminodiacetic acid resin, the Amberlite® IRC 748, known for its high
25 selectivity for heavy metals cations [27], and an acidic resin, the Amberlite® IR 120, which
26 could be selective depending on the eluent used [28]. Extraction rates of these resins were

1 studied using a multi-metal solution at pH=7, with a concentration of 10 $\mu\text{mol.L}^{-1}$ for each metal
2 and a flow rate of 2 mL.min^{-1} .

3 The results obtained with the Amberlite® IRC 748 were unsatisfactory: only 48% of cadmium
4 were extracted, while for interfering cations, 33% of calcium and 80% of zinc were extracted.
5 In addition, the various eluents tested (nitric acid, potassium iodide, ammonium nitrate and
6 ammonium oxalate) did not improve the selectivity for cadmium over interfering cations.

7 For the Amberlite® IR 120, the extraction step was more efficient for cadmium with an
8 extraction of 65%, but also for calcium and zinc, with an extraction yield of 70 and 85%
9 respectively. However, the elution step was crucial for the selective preconcentration of
10 cadmium. Many eluents at different concentrations have been tested and the most significant
11 results are resumed in Figure 3. Elution with nitric acid, ammonium nitrate and ammonium
12 oxalate did not present any selectivity for cadmium. In contrast, potassium iodide (KI 0.15
13 mol.L^{-1}) showed a significant selectivity for cadmium: 95% of cadmium was eluted, against
14 15% of calcium and 18% of zinc. Three concentrations of potassium iodide (0.05, 0.15 and 0.30
15 mol.L^{-1}) have then been tested in order to optimize cadmium elution. Less than 10% of
16 cadmium and other metals were eluted with KI 0.05 mol.L^{-1} . Cadmium was quantitatively
17 eluted at a rate of 95% with 0.15 and 0.30 mol.L^{-1} KI but with this last concentration, 30% of
18 calcium and about 40% of other metals such as Cu and Fe were also eluted. Thus, a
19 concentration of 0.15 mol.L^{-1} of potassium iodide was the most adequate to quantitatively elute
20 cadmium while limiting elution of interfering cations. Note that lead was previously extracted
21 by Triskem-Pb resin and therefore do not interfere in cadmium measurement.

22 Extraction and elution flow rates on Amberlite® IR 120 were tested between 1 and 6 mL.min^{-1}
23 ¹. Results showed that the best compromise between extraction/elution rates and analysis
24 duration was obtained when flow rate was fixed at 4 mL.min^{-1} . Flow rates above 4 mL.min^{-1}
25 resulted in small bubbles introduction in the flow system.

1

2 3.3.2. *Interfering cations during cadmium detection*

3 The extraction and elution steps on Amberlite® IR 120 eliminated the majority of interfering
4 cations. Less than 15% zinc was extracted and eluted and, given zinc levels usually found in
5 natural waters and the response of zinc with Rhod-5N, this element does not interfere with the
6 measurement of cadmium.

7 With the previously described procedure, 10% of calcium was finally extracted and eluted: in
8 the light of the high calcium levels usually found in natural waters, this quantity could still
9 interfere during the cadmium detection step. In these conditions, a procedure to quantify
10 separately calcium and determinate a signal correction for cadmium determination has been
11 established.

12 After a first step of extraction and elution of the two resins, cadmium and calcium are quantified
13 by Rhod-5N reagent. The fluorescence signal obtained thus corresponds to the concentration of
14 cadmium in the sample to which is added the interference of calcium. The sample is then
15 injected into the flow system a second time for a new extraction/elution cycle on both resins. A
16 masking agent solution of N,N,N',N'-tetrakis-(2-pyridylmethyl)ethylenediamine (TPEN) is
17 then added to Rhod-5N reagent and used to complex cadmium eluted [29]. The complex
18 cadmium-TPEN has a stability constant higher than those of cadmium-Rhod-5N [26,30] ($\log K_{Cd-TPEN}=17$; $\log K_{Cd-Rhod-5N}=8.85$). The fluorescence signal obtained thus allow the specific
19 quantification of calcium in sample. From this value, the fluorescence signal obtained
20 previously for the sum of cadmium and calcium can be corrected, and the cadmium
21 concentration can be determined separately. This correction can be applied to correct calcium
22 interference up to 400 mg.L^{-1} .

24

25 3.4. Analytical features

1 Main analytical features of the system developed are summarized in Table S1 (Supplementary
2 Materials). For cadmium analysis, a calibration curve has been constructed with a sample
3 volume of 5 mL. Domain range was linear between 0.2 and 15 $\mu\text{g.L}^{-1}$, with a limit of detection
4 (LOD; 3σ ; $n=10$) of 0.2 $\mu\text{g.L}^{-1}$ and a coefficient of variation (CV; $n=8$) of 3.0%. For lead, a
5 sample volume of 10 mL has been used, and a linear domain range has been obtained between
6 0.17 and 20 $\mu\text{g.L}^{-1}$, with a LOD of 0.17 $\mu\text{g.L}^{-1}$ and a CV of 6.2%. The sample volume can be
7 increased to improve the detection limit and thus allow the analysis of fresh waters with very
8 low concentrations of lead and cadmium, but to avoid interferences, the calcium content should
9 not exceed 0.4 mg.mL^{-1} in the sample. The complete analysis time for the sequential
10 determination of cadmium and lead is 18 minutes allowing the analysis of 3 samples per hour.
11 Santos et al. [18] have recently compared sequential injection methods for the biparametric
12 determination of cadmium and lead in water samples. In this study this comparison has been
13 extended to other flow systems and updated. Main analytical features of these previously
14 reported flow systems are compared in Table 2 with analytical performances of the proposed
15 3D-printed lab-on-valve system. Some of these works required an atomic absorption
16 spectrometer as a detector (with or without preconcentration step), resulting in low limits of
17 detection [31,32,33] but these detection techniques are not compatible with compact systems.
18 On another hand, some systems based on voltammetric techniques show good limit of detection
19 with large dynamic range and use of compact detection systems [34,35] but require complex
20 protocols for the preparation of electrodes. Systems using spectrometry as a detection method
21 have high detection limits [36] and the only LOV system to our best knowledge that has been
22 developed for the biparametric detection of cadmium and lead has thus been applied to the
23 screening of these metals in contaminated waters [18]. The MSFIA-LOV with fluorimetric
24 detection proposed in this study makes it possible to find a compromise between the criteria of
25 sensitivity, simplicity and cost. The LODs obtained (0.20 and 0.17 $\mu\text{g.L}^{-1}$ for cadmium and lead

1 respectively) are lower than the MAC-EQS (maximal allowable concentration-environmental
2 quality standards) as defined by the European regulations [37] (0.45 and 7.2 $\mu\text{g.L}^{-1}$ in inland
3 surface waters for cadmium and lead respectively) and thus allow determinations of lead and
4 cadmium in natural waters.

5

6 3.5. Validation

7 To validate the 3D printed LOV-MSFIA system, three samples of natural waters have been
8 collected in different locations in the Marseille city area (south-east of France). The samples
9 were filtered on a 0.45 μm polyethersulfone membrane and then UV-photooxidized at 254 nm
10 during 30 minutes before analysis allowing liberation of cadmium and lead linked to natural
11 organic ligands, inorganic ligands or even to anthropogenic organic ligands. The samples were
12 analyzed in duplicate by the developed 3D printed LOV-MSFIA system and by AAS. The
13 results are summarized in Table 3. The values obtained by the two methods were consistent.
14 For lead, the mean difference between the two methods was 1.8%, (min -6.8%; max 7.3%). The
15 results obtained for lead determination by the proposed system were compared (*t* test) with the
16 reference method values (AAS) and no significant differences at the 95% confidence level were
17 found. For cadmium, as the levels were below the LOD, samples were spiked to 5 $\mu\text{g.L}^{-1}$. The
18 results show an average underestimation of the cadmium content of 13%. These results can be
19 explained by the developed procedure which requires signal correction as a function of calcium
20 concentration.

21

22 **Conclusion**

23 A 3D printed LOV-MSFIA system has been developed to quantify lead and cadmium in natural
24 waters. Many 3D printing technologies have been tested to create the LOV unit, and digital
25 light processing seems to be the most adapted. Lead was selectively extracted on Triskem Pb

1 resin and eluted with ammonium oxalate. Cadmium was preconcentrated on Amberlite® IR
2 120 and selectively eluted with potassium iodide. These two metals were detected with Rhod-
3 5N fluorescent reagent. Detection limits obtained ($0.20 \mu\text{g.L}^{-1}$ for cadmium and $0.17 \mu\text{g.L}^{-1}$ for
4 lead) were compatible with analysis of lead and cadmium in fresh or brackish waters. The
5 demonstration of the use of 3D printing for the manufacture of LOV units opens new
6 perspectives for the design of more complex LOV systems.

7

8 **Acknowledgment**

9 This work was included in the project “Lab-on-Ship” funded by the French Research Agency
10 (ANR-14-CE04-0004).

11

12 **References**

13

- 14 [1] R. Vigneri, P. Malandrino, F. Gianì, M. Russo, P. Vigneri, Heavy metals in the volcanic
15 environment and thyroid cancer, *Molecular and Cellular Endocrinology*. 457 (2017) 73–
16 80. doi:10.1016/j.mce.2016.10.027.
- 17 [2] X. Shao, H. Cheng, Q. Li, C. Lin, Anthropogenic atmospheric emissions of cadmium in
18 China, *Atmospheric Environment*. 79 (2013) 155–160.
19 doi:10.1016/j.atmosenv.2013.05.055.
- 20 [3] M.P. Taylor, S.A. Mould, L.J. Kristensen, M. Rouillon, Environmental arsenic,
21 cadmium and lead dust emissions from metal mine operations: Implications for
22 environmental management, monitoring and human health, *Environ. Res.* 135 (2014)
23 296–303. doi:10.1016/j.envres.2014.08.036.

- 1 [4] M. Pecht, Y. Fukuda, S. Rajagopal, The impact of lead-free legislation exemptions on
2 the electronics industry, *IEEE Transactions on Electronics Packaging Manufacturing*.
3 27 (2004) 221–232. doi:10.1109/TEPM.2004.843150.
- 4 [5] H. Galal-Gorchev, Dietary intake of pesticide residues: Cadmium, mercury, and lead,
5 *Food Additives and Contaminants*. 8 (1991) 793–806.
6 doi:10.1080/02652039109374038.
- 7 [6] P. Mushak, Chapter 26 - Lead Regulation and Regulatory Policies: Lead in Paint, in:
8 *Trace Metals and Other Contaminants in the Environment*, Elsevier, 2011: pp. 841–873.
9 doi:10.1016/B978-0-444-51554-4.00026-2.
- 10 [7] WHO, Cadmium, WHO. (n.d.).
11 http://www.who.int/ipcs/assessment/public_health/cadmium/en/ (accessed December
12 8, 2017).
- 13 [8] A. Wilk, E. Kalisińska, D.I. Kosik-Bogacka, M. Romanowski, J. Róžański, K.
14 Ciechanowski, M. Słojewski, N. Łanocha-Arendarczyk, Cadmium, lead and mercury
15 concentrations in pathologically altered human kidneys, *Environmental Geochemistry*
16 *and Health*. 39 (2017) 889–899. doi:10.1007/s10653-016-9860-y.
- 17 [9] S.C. Larsson, A. Wolk, Urinary cadmium and mortality from all causes, cancer and
18 cardiovascular disease in the general population: systematic review and meta-analysis
19 of cohort studies, *Int J Epidemiol*. 45 (2016) 782–791. doi:10.1093/ije/dyv086.
- 20 [10] WHO, Lead poisoning and health, WHO. (n.d.).
21 <http://www.who.int/mediacentre/factsheets/fs379/en/> (accessed November 10, 2016).
- 22 [11] S. Cerutti, M.F. Silva, J.A. Gásquez, R.A. Olsina, L.D. Martinez, On-line
23 preconcentration/determination of cadmium in drinking water on activated carbon using
24 8-hydroxyquinoline in a flow injection system coupled to an inductively coupled plasma

- 1 optical emission spectrometer, *Spectrochimica Acta Part B: Atomic Spectroscopy*. 58
2 (2003) 43–50. doi:10.1016/S0584-8547(02)00215-X.
- 3 [12] L.O.B. Silva, L.A. Portugal, E. Palacio, L. Ferrer, V. Cerdà, S.L.C. Ferreira, Multi-
4 commuted flow system for cadmium determination in natural water by cold vapour
5 atomic absorption spectrometry, *J. Anal. At. Spectrom.* 29 (2014) 2398–2404.
6 doi:10.1039/C4JA00305E.
- 7 [13] A.C.M. Aleluia, F.A. de Santana, G.C. Brandao, S.L.C. Ferreira, Sequential
8 determination of cadmium and lead in organic pharmaceutical formulations using high-
9 resolution continuum source graphite furnace atomic absorption spectrometry,
10 *Microchemical Journal*. 130 (2017) 157–161. doi:10.1016/j.microc.2016.09.001.
- 11 [14] J. Ruzicka, Lab-on-valve: universal microflow analyzer based on sequential and bead
12 injection, *The Analyst*. 125 (2000) 1053–1060. doi:10.1039/b001125h.
- 13 [15] S.S.M.P. Vidigal, I.V. Tóth, A.O.S.S. Rangel, Sequential injection lab-on-valve
14 platform as a miniaturisation tool for solid phase extraction, *Anal. Methods*. 5 (2013)
15 585–597. doi:10.1039/C2AY26322J.
- 16 [16] I.C. Santos, R.B.R. Mesquita, A.O.S.S. Rangel, Micro solid phase spectrophotometry in
17 a sequential injection lab-on-valve platform for cadmium, zinc, and copper
18 determination in freshwaters, *Analytica Chimica Acta*. 891 (2015) 171–178.
19 doi:10.1016/j.aca.2015.08.021.
- 20 [17] A. González, R.B.R. Mesquita, J. Avivar, T. Moniz, M. Rangel, V. Cerdà, A.O.S.S.
21 Rangel, Microsequential injection lab-on-valve system for the spectrophotometric bi-
22 parametric determination of iron and copper in natural waters, *Talanta*. (2017).
23 doi:10.1016/j.talanta.2017.02.055.

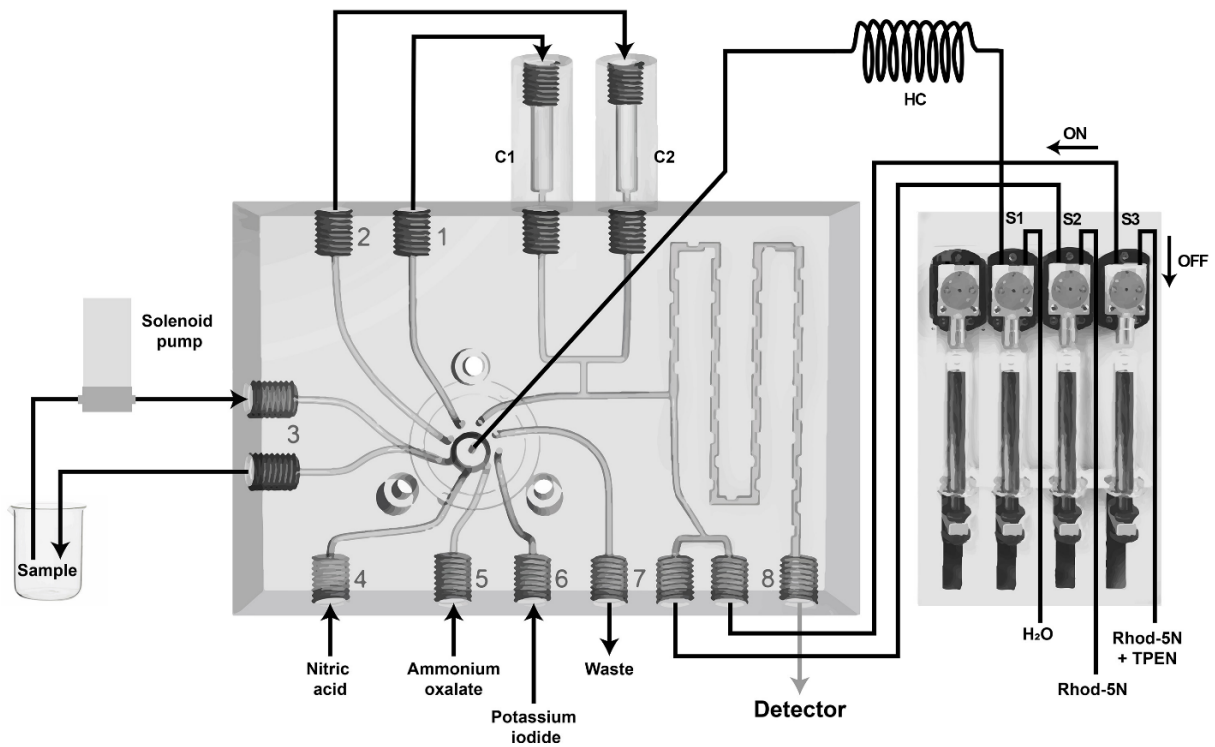
- 1 [18] I.C. Santos, R.B.R. Mesquita, A.O.S.S. Rangel, Screening of cadmium and lead in
2 potentially contaminated waters using a spectrophotometric sequential injection lab-on-
3 valve methodology, *Talanta*. 143 (2015) 359–365. doi:10.1016/j.talanta.2015.05.005.
- 4 [19] N.P. Macdonald, J.M. Cabot, P. Smejkal, R.M. Guijt, B. Paull, M.C. Breadmore,
5 Comparing microfluidic performance of 3D printing platforms, *Anal. Chem.* (2017).
6 doi:10.1021/acs.analchem.7b00136.
- 7 [20] C. Chen, B.T. Mehl, A.S. Munshi, A.D. Townsend, D.M. Spence, R.S. Martin, 3D-
8 printed microfluidic devices: fabrication, advantages and limitations—a mini review,
9 *Anal. Methods*. 8 (2016) 6005–6012. doi:10.1039/C6AY01671E.
- 10 [21] N. Bhattacharjee, A. Urrios, S. Kang, A. Folch, The upcoming 3D-printing revolution
11 in microfluidics, *Lab Chip*. 16 (2016) 1720–1742. doi:10.1039/C6LC00163G.
- 12 [22] A.A. Yazdi, A. Popma, W. Wong, T. Nguyen, Y. Pan, J. Xu, 3D printing: an emerging
13 tool for novel microfluidics and lab-on-a-chip applications, *Microfluidics and*
14 *Nanofluidics*. 20 (2016). doi:10.1007/s10404-016-1715-4.
- 15 [23] C. Calderilla, F. Maya, V. Cerdà, L.O. Leal, 3D printed device including disk-based
16 solid-phase extraction for the automated speciation of iron using the multisyringe flow
17 injection analysis technique, *Talanta*. 175 (2017) 463–469.
18 doi:10.1016/j.talanta.2017.07.028.
- 19 [24] E. Mattio, F. Robert-Peillard, C. Branger, K. Puzio, A. Margailan, C. Brach-Papa, J.
20 Knoery, J.-L. Boudenne, B. Coulomb, 3D-printed flow system for determination of lead
21 in natural waters, *Talanta*. 168 (2017) 298–302. doi:10.1016/j.talanta.2017.03.059.
- 22 [25] J.F. García-Reyes, P. Ortega-Barrales, A. Molina-Díaz, Sensing of trace amounts of
23 cadmium in drinking water using a single fluorescence-based optosensor,
24 *Microchemical Journal*. 82 (2006) 94–99. doi:10.1016/j.microc.2005.11.001.

- 1 [26] M. Soibinet, V. Souchon, I. Leray, B. Valeur, Rhod-5N as a Fluorescent Molecular
2 Sensor of Cadmium(II) Ion, *Journal of Fluorescence*. 18 (2008) 1077–1082.
3 doi:10.1007/s10895-008-0352-z.
- 4 [27] A.F. Shaaban, D.A. Fadel, A.A. Mahmoud, M.A. Elkomy, S.M. Elbahy, Removal of
5 Pb(II), Cd(II), Mn(II), and Zn(II) using iminodiacetate chelating resin by batch and
6 fixed-bed column methods, *Desalination and Water Treatment*. 51 (2013) 5526–5536.
7 doi:10.1080/19443994.2012.758059.
- 8 [28] R. Přibil, V. Veselý, The extraction separation of cadmium and zinc and their
9 complexometric determination in the presence of other elements, *Collect. Czech. Chem.*
10 *Commun., CCCC*. 37 (1972) 13–21. doi:10.1135/cccc19720013.
- 11 [29] M. Ohkubo, A. Miyamoto, M. Shiraishi, Heavy metal chelator TPEN attenuates fura-2
12 fluorescence changes induced by cadmium, mercury and methylmercury, *Journal of*
13 *Veterinary Medical Science*. 78 (2016) 761–767.
- 14 [30] C.A. Blindauer, M.T. Razi, S. Parsons, P.J. Sadler, Metal complexes of N,N,N',N'-
15 tetrakis(2-pyridylmethyl)ethylenediamine (TPEN): Variable coordination numbers and
16 geometries, *Polyhedron*. 25 (2006) 513–520. doi:10.1016/j.poly.2005.08.019.
- 17 [31] A.N. Anthemidis, K.-I. G. Ioannou, Development of a sequential injection dispersive
18 liquid–liquid microextraction system for electrothermal atomic absorption spectrometry
19 by using a hydrophobic sorbent material: Determination of lead and cadmium in natural
20 waters, *Analytica Chimica Acta* 668 (2010) 35-40. doi:10.1016/j.aca.2009.10.063.
- 21 [32] Z.H. Wang, Z.P. Zhang, Z.P. Wang, L.W. Liu, X.P. Yan, Acrylic acid grafted
22 polytetrafluoroethylene fiber as new packing for flow injection on-line microcolumn
23 preconcentration coupled with flame atomic absorption spectrometry for determination
24 of lead and cadmium in environmental and biological samples, *Analytica Chimie Acta*
25 514 (2004) 151-157. doi:10.1016/j.aca.2004.03.049.

- 1 [33] A. N.Anthemidis, G.G.S. Xidia, M. Miró, On-line sorptive preconcentration platform
2 incorporating a readily exchangeable Oasis HLB extraction micro-cartridge for trace
3 cadmium and lead determination by flow injection–flame atomic absorption
4 spectrometry, *Microchemical Journal* 98 (2011) 66-71.
5 doi.org/10.1016/j.microc.2010.11.007.
- 6 [34] B. Nimwong, S. Chuanuwatanakul, O. Chailapakul, W. Dungchai, S. Motomizu, On-
7 line preconcentration and determination of lead and cadmium by sequential
8 injection/anodic stripping voltammetry, *Talanta* 96 (2012) 75-81.
9 doi:10.1016/j.talanta.2012.03.057.
- 10 [35] W. Wonsawatt, S. Chuanuwatanakul, W. Dungchai, E. Punrat, S. Motomizu, O.
11 Chailapakul, Graphene-carbon paste electrode for cadmium and lead ion monitoring in
12 a flow-based system, *Talanta* 100 (2012) 282-289. doi:10.1016/j.talanta.2012.07.045.
- 13 [36] J.F.van Staden, R.E.Taljaard, Determination of Lead(II), Copper(II), Zinc(II),
14 Cobalt(II), Cadmium(II), Iron(III), Mercury(II) using sequential injection extractions,
15 *Talanta* 64 (2004) 1203-1212. doi.org/10.1016/j.talanta.2004.06.020.
- 16 [37] Directive 2008/105/EC of the European parliament and of the council of 16 December
17 2008 on environmental quality standards in the field of water policy, amending and
18 subsequently repealing Council Directives 82/176/EEC, 83/513/EEC, 84/156/EEC,
19 84/491/EEC, 86/280/EEC and amending Directive 2000/60/EC of the European
20 Parliament and of the Council. <http://data.europa.eu/eli/dir/2008/105/oj>.
- 21 [38] V. Guzsvány, H. Nakajima, N. Soh, K. Nakano, T. Imato, Antimony-film electrode for
22 the determination of trace metals by sequential-injection analysis/anodic stripping
23 voltammetry, *Analytica Chimica Acta* 658 (2010) 12–17.
24 doi:10.1016/j.aca.2009.10.049.

- 1 [39] S. Suteerapataranon, J. Jakmune, Y. Vaneesorn, K. Grudpan, Exploiting flow injection
2 and sequential injection anodic stripping voltammetric systems for simultaneous
3 determination of some metals, *Talanta* 58 (2002) 1235-1242.
- 4 [40] E.L. Silva, P. dos Santos Roldan, Simultaneous flow injection preconcentration of lead
5 and cadmium using cloud point extraction and determination by atomic absorption
6 spectrometry, *Journal of Hazardous Materials* 161 (2009) 142–147.
7 doi:10.1016/j.jhazmat.2008.03.100.
- 8 [41] T. Yamane, Y. Yamaguchi, Complex formation of 2-(5-nitro-2-pyridylazo)-5-(N-
9 propyl-N-sulfo-propylamino)phenol with lead, cadmium and manganese for their
10 sensitive spectrophotometric detection in flow injection and ion chromatography
11 systems, *Analytica Chimie Acta* 345 (1997) 139-146.
- 12 [42] W. Siringkhawut, S. Pencharee, K. Grudpan, J. Jakmune, Sequential injection
13 monosegmented flow voltammetric determination of cadmium and lead using a bismuth
14 film working electrode, *Talanta* 79 (2009) 1118-1124.
15 doi:10.1016/j.talanta.2009.03.032.
- 16
17

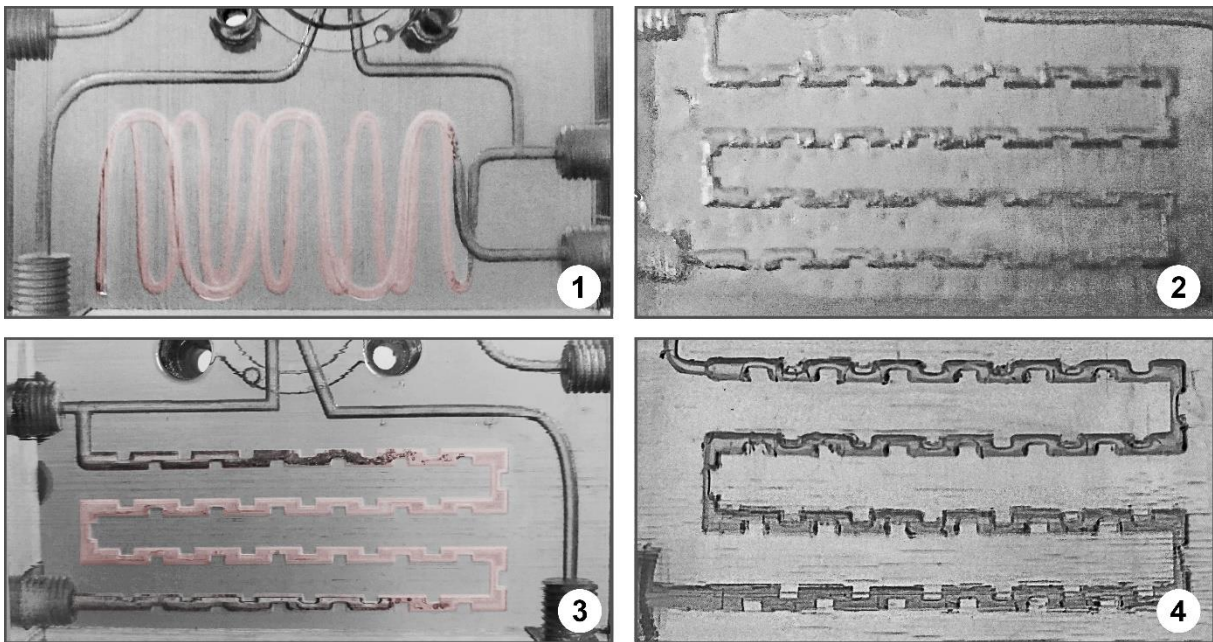
1



2

3 Figure 1. MSFIA-LOV system used for cadmium and lead determination with C1 column for
4 lead extraction and C2 column for cadmium.

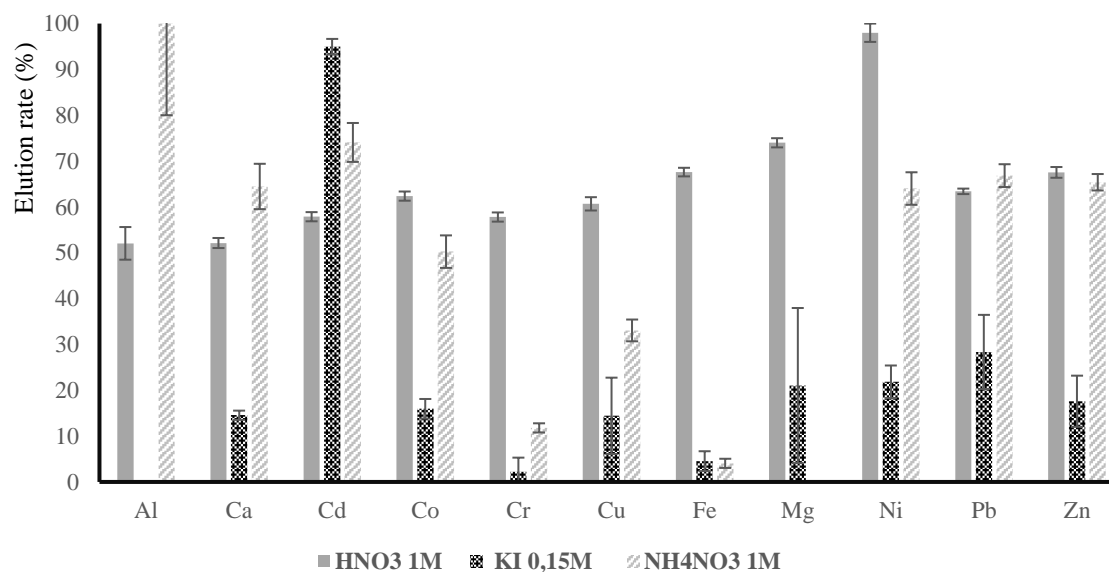
5



6

7 Figure 2. Mixing coils printed with different technologies: Polyjet (1;3), Stereolithography
8 (2), DLP (4).

1



2 Figure 2. Elution rate of a multi-metal solution ($10 \mu\text{mol.L}^{-1}$ for each metal) on Amberlite® IR
 3 120 H with different eluents.

4

5 Table 1. Flow procedure for cadmium and lead determination.

Step	LOV position	Volume (mL)	Flow-rate (mL/min)	S1	S2	S3	
Conditioning TrisKem Pb resin (C1)							
1	Loading HNO ₃	4	4	ON	OFF	OFF	
2	Dispensing HNO ₃ towards C1	1	4	ON	OFF	OFF	
Sample loading							
3	Loading sample into HC	3	5	4	ON	OFF	OFF
4	Dispensing sample into C1	1	5	4	ON	OFF	OFF
5	Loading previous sample into HC	8	5	4	ON	OFF	OFF
6	Dispensing previous sample into C2	2	5	4	ON	OFF	OFF
Elution of Amberlite® IR 120 (C2) and cadmium detection							
7	Loading potassium iodide into HC	6	4	4	ON	OFF	OFF
8	Simultaneous dispensing of potassium iodide into C2 and Rhod-5N into mixing coil	2	4	4	ON	ON	OFF
Sample loading through							
9	Loading sample into HC	3	5	4	ON	OFF	OFF

10	Dispensing sample into C1	1	5	4	ON	OFF	OFF
11	Loading previous sample into HC	8	5	4	ON	OFF	OFF
12	Dispensing previous sample into C2	2	5	4	ON	OFF	OFF
Interferences integration for Cd							
13	Loading potassium iodide	6	4	4	ON	OFF	OFF
14	Simultaneous dispensing potassium iodide into C2 and Rhod-5N with TPEN into mixing coil	2	4	4	ON	OFF	ON
Interferences elimination for Pb							
15	Loading HNO ₃	4	4	4	ON	OFF	OFF
16	Dispensing HNO ₃ to C1	1	4	4	ON	OFF	OFF
Elution of TrisKem Pb (C1) and lead detection							
17	Loading ammonium oxalate	5	4	4	ON	OFF	OFF
18	Simultaneous dispensing ammonium oxalate into C1 and Rhod-5N into mixing coil	1	4	4	ON	ON	OFF

1

2

1 Table 2. Comparison of main analytical features of flow systems for cadmium and lead
 2 determination in water samples.
 3

Flow system	Detection	Pb Range ($\mu\text{g}\cdot\text{L}^{-1}$)	Pb LOD ($\mu\text{g}\cdot\text{L}^{-1}$)	Cd Range ($\mu\text{g}\cdot\text{L}^{-1}$)	Cd LOD ($\mu\text{g}\cdot\text{L}^{-1}$)	Matrix	Ref.
SI-DLLME	ETAAS	0.04-1.5	0.01	0.006-0.15	0.002	Natural waters	[31]
SI	ASV	0.5-15	0.01	0.5-15	0.01	Tap water	[34]
SI	CV or SWASV	0.1-50	0.04	0.1-50	0.07	Tap water	[35]
MSFIA-LOV	Fluorimetry	0.2-15	0.17	0.2-20	0.20	Natural waters	This work
FI	FAAS	2.5-250	0.26	0.5-60	0.1	HNO ₃ extracts of biological and environmental samples	[32]
FI	FAAS	3.1-200	0.92	0.3-12	0.09	Water samples	[33]
SI	ASV	4.7-120	1.5	5.2-110	1.7	Tap water	[38]
FI	ASV	10-100	2	10-30	1	Wastewater samples	[39]
FI	CPE-FAAS	50-250	4.5	5-25	0.75	Water samples	[40]
FI	IC-PCR-PAD	0-300	4.8	0-150	1.9	Food samples after microwave digestion	[41]
SI-MSFA	ASV	10-100	6.9	10-100	1.4	Water samples	[42]
SI	ASV	10-100	10	10-70	6	Wastewater samples	[39]
SI-LOV	Spectrometry	500-10000	56	500-10000	34	Contaminated waters	[18]
SI	Spectrometry	1000-20000	-	1000-5000	-	Tap water	[36]

1 FI, flow injection; SI, sequential injection; SI-MSFA, sequential injection-monosegmented
 2 flow analysis; SI-DLLME, sequential injection-dispersive liquid-liquid microextraction; SI-
 3 LOV, sequential injection-lab-on-valve; MSFIA-LOV, multisyringe flow injection analysis-
 4 lab-on-valve; SV, anodic stripping voltammetry; CV, cyclic voltammetry; SWASV, square
 5 wave anodic stripping voltammetry; FAAS, flame atomic absorption spectrometry; IC-PCR-
 6 PAD, ion chromatography-post column reaction-photodiode array detector, ETAAS,
 7 electrothermal atomic absorption spectrometry; CPE-FAAS, cloud point extraction-flame
 8 atomic absorption spectrometry.

9

10 Table 3. Lead and cadmium determination in natural waters with 3D printed LOV-MSFIA
 11 system.

12

Samples	Lead ($\mu\text{g/L}$)		Cadmium ($\mu\text{g/L}$)	
	3D LOV-MSFIA	AAS	3D LOV-MSFIA	3D LOV-MSFIA Spiked to 5 $\mu\text{g/L}$
Spring water	11.7 ± 0.4	10.9 ± 0.5	< LOD	4.4 ± 0.6
City canal water	6.9 ± 0.5	7.4 ± 0.6	< LOD	4.1 ± 0.3
Well water	11.1 ± 0.3	11.8 ± 0.4	< LOD	4.5 ± 0.5

13

14